

A Polyphase Filter Bank Interpretation of Coherent Image Formation

C. Bhattacharya

DEAL (DRDO), Dehradun-248 001

e-mail: dealdrdo@del2.vsnl.net.in

Abstract

Coherent image formation in step transform algorithm is realized by overlapped subapertures in both range and cross range direction. Subaperture formation principle is treated as multiplication of target backscatter signature with a set of overlapped and shifted complex, conjugate reference functions and subsequent spectral analysis. A polyphase filter bank interpretation of step transform is presented here from Joint Time (space) Frequency (JTF) analysis viewpoint. Real time image formation is facilitated by such interpretation. Simulation results from such analysis are provided in the paper.

I. Introduction

Coherent image formation with overlapped subapertures as in Synthetic Aperture Radar (SAR) is widely reported and realized. Variations in the overlapped subaperture algorithm are known as Deramp-FFT, step transform, SPECAN, etc. In all these approaches the subaperture formation principle is treated as multiplication of target backscatter signature with a set of overlapped and shifted complex, conjugate reference functions and subsequent spectral analysis. Coherent integration for fine resolution image formation is done at the second stage after necessary quadratic phase correction. Such methods are particularly attractive for airborne sensors with negligible range migration costs and real time image formation possibilities [7], [12].

Detailed analysis of step transform algorithm appeared in [3], [10]; filter bank realization of subapertures using step transform are described in [6], [9]. Although polyphase filter banks appear in [9], no analysis is given for image formation with such filter banks. Real time subaperture formation has been reported in [6], [7] using overlap among subapertures in the frequency domain and linear approximation of quadratic phase correction. One major drawback in step transform is aliasing among coarse resolution frequency bin output samples that produce invalid data during fine resolution processing. Chirp-z transform has been offered as a solution against such aliasing in recent literature [5], [13].

SAR image formation is a case of Joint Time (space) Frequency (JTF) analysis where point target signature in the image is the Impulse Response Function (IRF) for a 2-dimensional range variant matched filter. Range-doppler imaging for rotating objects has been interpreted by JTF analysis [2]. A detailed analysis of step transform in

polyphase filter bank formation appeared in [1] including range migration correction. More recently, step transform has been treated in time varying subaperture formation to counter large range migration due to high squint [11]. But these analyses do not point to JTF character of SAR focusing. Here we provide a systematic analysis of step transform algorithm from JTF viewpoint for strip-map SAR image formation. The analysis results in polyphase filter bank realization with several pointers for real time image formation as described in the paper.

In section II we present JTF analysis for step transform comparing with methods given in [9], [10]. We make several simplifying assumptions to stress on the basic image formation process, such as no motion compensation, no range migration correction and uniform antenna gain over beam width. These assumptions are compatible with the simulation parameters chosen. Simulation parameters and results are given in section III; section IV draws the conclusion of the paper.

II. JTF Analysis of Step Transform Algorithm

In the following analysis 2-dimensional matched filter model of strip-map SAR is represented as two consecutive 1-dimensional correlators, which fits the case of air-borne sensor model as ground foot print is small enough to circumvent range cell migration correction [8]. The point target backscatter in that case is dispersed both in fast-time (t) and slow-time (s) chirps and is represented as [3],

$$v_r(s, t) = \exp[-j4\pi R(s)/\lambda] \exp[jf(t - 2R(s)/c)] \\ \text{with } |t - 2R(s)/c| \leq \tau_p/2 \quad (1)$$

Here $R(s)$ is the range to the broadside target at slow-time index s ; τ_p is the pulse length of transmission and c being velocity of light. The correlator function in fast time t is replica of the transmitted chirp, $f(t)$ and is given by,

$$f(t) = \exp[j\pi K t^2] \text{rect}(t/\tau_p) \\ \text{with } \text{rect}(t/\tau_p) = 1, |t| \leq \tau_p/2 \\ = 0, \text{elsewhere} \quad (2)$$

Here K is rate of frequency sweep in pulse duration τ_p . In slow time the correlator function $S(s)$ is the quadratic phase variation model derived from sensor-ground patch geometry in space. For broadside targets, $S(s)$ is expressed as [3],

$$S(s) = \exp[-j4\pi(R_0 - (\lambda/2)f_R s^2)/\lambda] \text{rect}(s/\tau_{int})$$

with $f_R = \ddot{R}(s)|_{s=0}$, gradient of range rate;

$$= -2V_p^2/\lambda R_0; V_p \text{ is platform velocity}; \quad (3)$$

Here λ is the wavelength of transmission and R_0 is the broadside range at phase center of backscatter signal. Coherent integration interval is τ_{int} considering uniform antenna gain over finite beam width. Equation (3) shows the range dependent nature of cross-range correlator.

II A. Coarse Resolution Analysis

In step transform, overlapped subapertures substitute the correlator functions and approximate the IRF as shown in the block diagram of Fig.1. Advantages are much smaller DFT size, realization of overlapped subapertures by parallel processing in DFT filter bank [6].

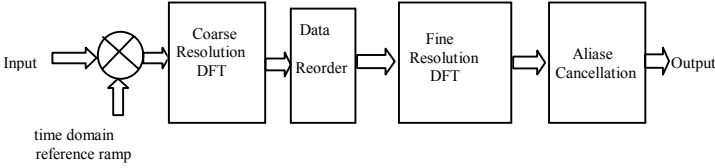


Fig.1 Step Transform in range direction adapted from [10].

The coarse resolution transform in range direction is shown in [10] as,

$$F(q) = \sum_{k=0}^{T/\Delta-1} w_1(k) v_r(s, k) f_1^*(k) \exp[-j(2\pi\Delta/T)kq] \quad (4)$$

Here $f_1(k)$ is the discrete, reference chirp function of duration T sampled at Δ interval in fast time. This is generated by periodic ramp chirp generator as shown in Fig.1.

$$f_1(k) = \exp[j\pi K(k-n)^2 \Delta^2] \quad (5)$$

with k being local index for reference chirp and

$$n\Delta = (i+A)N\Delta,$$

is the position of i^{th} reference chirp, $N\Delta$ being the overlap interval with first subaperture occurring at $A\Delta$ time. $w_1(k)$ is the window used for sidelobe suppression.

The same process may be expressed as multiplication by a complex, gaussian, sliding window and subsequent DFT operation. We consider a complex, gaussian window, $g(l\Delta)$ as,

$$g(l\Delta) = \exp[j\pi K(l\Delta)^2], \quad |l\Delta| \leq T/2$$

$$= 0, \quad \text{elsewhere}, \quad \infty < l\Delta < \infty \quad (6)$$

Discrete samples of received signal $v_r(s, l)$ for a certain slow time index s can be written from the discrete version of equation(1) as,

$$v_r(s, l\Delta) = \exp[-j4\pi R(s)/\lambda] \exp[j\pi K(l\Delta - m\Delta)^2];$$

Ignoring the constant phase term in $v_r(s, l)$ for a definite pulse duration ($2R(s)/c = m\Delta$) and with the window placed at $n\Delta$, step transform may be expressed as,

$$V_r((n-m), \omega_q) = \sum_{l=-\infty}^{\infty} v_r(s, l\Delta) g^*(l\Delta - n\Delta) \exp(-j\omega_q l)$$

$$= \sum_{l=-\infty}^{\infty} \exp[j\pi K(l-m)^2 \Delta^2] \times$$

$$\exp[-j\pi K(n-l)^2 \Delta^2] \exp(-j\omega_q l)$$

Let $(l-m) = c$; then $(n-l) = (n-m)-c$;

$$V_r((n-m), \omega_q) = \exp(-j\omega_q m) \sum_{c=-\infty}^{\infty} \exp[j\pi K(c\Delta)^2] \times$$

$$\exp[-j\pi K(n-m-c)^2 \Delta^2] \exp(-j\omega_q c) \quad (7)$$

The expression in equation (7) is the Short Time Fourier Transform (STFT) of signal $v_r(s, l)$ in range direction associated with a phase term $\exp(-j\omega_q m)$, $0 \leq q \leq (M-1)$.

Compared to equation (4) the limits of integration are changed to infinity to represent the STFT expression; this conforms to the condition here, as the target backscatter is received for finite duration in both fast and slow time dimensions. With no loss of generality the window function $g(l\Delta)$ is premultiplied by $w_1(l\Delta)$ to minimize sidelobe aliasing of the STFT sequences.

Equation (7) represents JTF analysis in range direction with fixed time, frequency grid. Grid interval in fast time is the overlap factor of shifted window, i.e. $M\Delta$ and frequency resolution is the inverse of duration T ; hence the analysis produces coarse resolution range bins. The IRF in coarse resolution is thus a 2-dimensional STFT of target backscatter.

Equation (7) may be represented as the output sequence of polyphase filter bank [4]. The spectrum analyzer in equation (7) is a filter bank expression. Polyphase decomposition is possible here as the window function has finite support both in time and frequency and the noble identity of decimation holds.

Polyphase filterbank decomposition, $V_q(z)$ is given by,

$$V_q(z) = \sum_{p=0}^{M-1} [z^{-p} G_{0p}(z^M) V_r^{\wedge}(z)] W_M^{-pq}, \quad 0 \leq q \leq (M-1)$$

$$\text{where } W_M = \exp(-j2\pi/M) \quad (8)$$

Here $G_{0p}(z)$ is the z -transform of the p^{th} polyphase component of $g(l\Delta)$. Specifically, $g_{0p}(l) = g(Ml+p)$; $V_r^{\wedge}(z)$ being the z -transform of $v_r(s, l)$ over index l . The inner bracket expression is performed in the time domain

polyphase filterbank followed by the IDFT operation as shown in Fig.2.

The STFT component of equation (7) is related to the filterbank output, $V_q(z)$ of equation(8) as,

$$STFT [v_r(s, l)] = W_M^{-q} V_q(\omega_q),$$

with $z = 2\pi(q/M)$

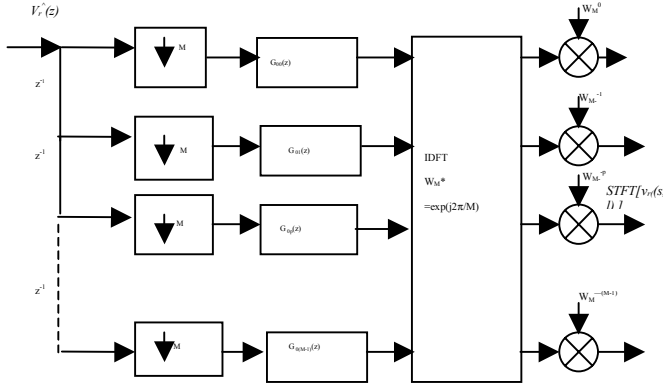


Fig.2 Polyphase filterbank representation of coarse resolution step transform

Equation (7) is modified to express coarse resolution frequency bin component, $V_r((n-m), \omega_q)$ in terms of maximally decimated filterbank output sequence as shown in Fig.2 as,

$$V_r((n-m), \omega_q) = \exp(-j\omega_q m) W_M^{-q} V_q(\omega_q) \quad (9)$$

Coarse resolution step transform as expressed in equation (9) is shown in block diagram form in Fig. 2.Fig.3. is the functional block diagram of step transform by JTF analysis.

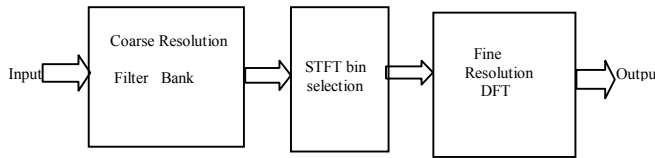


Fig.3 Step transform by polyphase filterbank

Some implications of this realization in Fig.3 are:

- Demand on the processor speed is reduced considerably as the processing is done at $1/M$ of the sampling rate as shown in Fig.2.
- Processing is done in real time as the polyphase filterbank has very low latency; filter bank operates in time domain with few coefficients.
- Spectral resolution ($1/T$) and coarse bin spectral separation ($1/MA$) are treated independent of each other; coarse frequency bin separation due to adjacent targets is large enough not to cause aliasing. It is to be noted that this property has also been realized in [9] by *fold FFT* operation.

- As a hardware item the ramp frequency generator for step transform in equation (4) is not needed as the window function $g(l\Delta)$ is realized as the impulse response of the filter bank.

In cross-range direction slow time variable s is inherently sampled at **Pulse Repetition Frequency (PRF)**. Phase of target backscatter as a function of range in the subaperture interval constitute the reference chirp as shown in equation (3). Position of a subaperture and phase variation in that interval for a broadside range R_0 are interlocked during formation of synthetic aperture making quadratic phase compensation in cross-range possible. This is shown in Fig.4 for the full synthetic aperture. The size of the subaperture (l) is related to the overlap factor, M by,

$$N_a = (N-1)M + l \quad (10)$$

Here N_a is the total number of pulse samples in slow time integration interval. Subaperture interval is small enough for skipping range cell migration correction. The number of subapertures, N is twice the number of looks desired for multilook processing.

IIB. Fine Resolution Analysis

Each STFT sequence from filterbank in Fig.2. represents a constant tone for duration T ; the amplitude of the tone gives target's presence. This complex response from a single coarse resolution bin repeats in the grid along the diagonal vectors of overlapped JTF matrix [3]. Coherent integration for full resolution is achieved by taking DFT over the phase of each diagonal vector of this JTF matrix after quadratic phase compensation depending on overlap interval M . Essentially it means data selection from coarse resolution analysis output for the tone corresponding to a single target; the resolution of this tone is determined by inverse of the duration ($1/T$) of coarse resolution window function $g(l\Delta)$. Thus the bandpass bandwidth of coarse resolution subaperture is resolved among fine resolution intervals of ($1/\tau_{int}$) resulting in fully focused synthetic aperture.

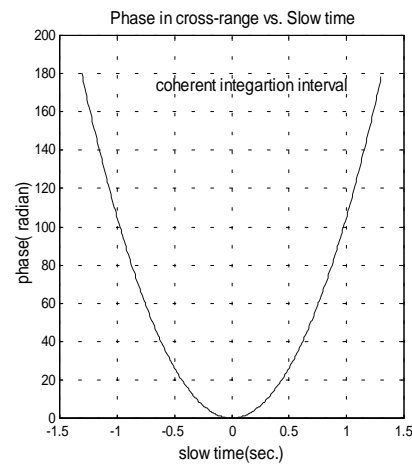


Fig.4 Cross-range phase variation vs. slow time

In practice the resolution is poorer than the DFT filter bandwidth because of the window chosen in suppressing the sidelobes of adjacent filters.

It is to be noted that the phase function $\exp(-j\omega_q m)$ in the JTF representation in equation(9) is a constant phase term because of periodic nature of ω_q along the diagonal vector of JTF matrix. The two dimensional elements of JTF matrix represent the overlap interval, $M\Delta$ and frequency bin ω_q respectively.

IV. Simulation

For fully focused SAR, the product of two 1-dimensional *sinc* functions, which are point target response from DFT filter banks in range and cross-range, is the IRF for point targets in 2-dimensions. The 2-dimensional IRF is expressed as,

$$v(s, t) = \sigma_{cr} \sigma_r \exp(-j 4\pi R_0 / \lambda) \times \sin c(\pi f_R^T \tau_{int} (s - s_0)) \sin c(\pi K T (t - t_0)) \quad (11)$$

Here σ_{cr} , σ_r are matched filter compression gains in cross-range and range direction respectively standing for amplitude of IRF function. The point target co-ordinate in the image is given by $(V_0 s_0, c/2t_0)$, mapped by the slow-time and fast-time velocity parameters respectively. The DFT filter response of equation (11) is widened by window multiplication to keep **Peak Sidelobe Ratio (PSLR)** at desired level. Here we use Gaussian window whose sidelobe suppression character is compared to DFT filter response in Fig.5.

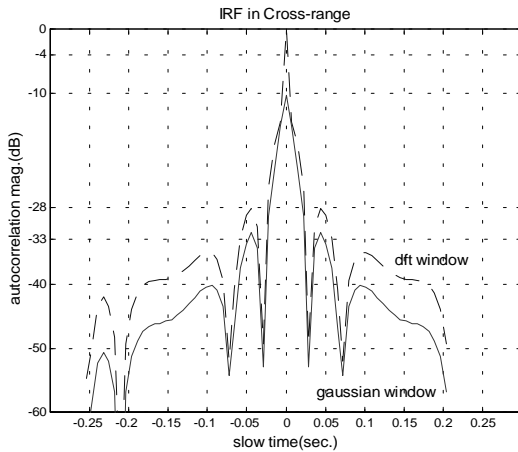


Fig.5 PSLR characteristics of Gaussian window

For negligible range migration, we take range curvature to be $1/4^{\text{th}}$ of range resolution size over the integration interval τ_{int} [3]; i.e.,

$$(\delta x / \lambda)^2 > R_0 / 8\delta R$$

It is seen that working with smaller wavelengths can avoid range migration curvature compensation provided cross-range resolution δx is of medium size ($\delta x > 1m$). We choose a

Ku-band frequency with the simultaneous advantage of higher antenna gain at smaller size. The simulation parameters chosen are given in Table1.

Table1. Simulation Parameters for Polyphase Step Transform

Parameter	Value	Units
Operating frequency (c/λ)	Ku band, 14.2	GHz
Nominal range (R_0)	8560	m
Aircraft velocity (V_0)	55	m
Pulse duration (τ_p)	10	microsec.
Bandwidth ($K\tau_p$)	60	MHz.
PRF	138	Hz
Coherent integration time (τ_{int})	3.28	sec
Fast time subaperture (T)	2.0	microsec.
Slow time subaperture	0.574	sec.
Fast time overlap (M)	60	samples
Slow time overlap	40	samples
PSLR	-35	dB
Windowed Range resol. ($2\delta R$)	5	m.
4-look Cross- range resol. ($4\delta x$)	2	m.

With these parameters, sampling frequency for complex target back scatter $v_r(s, t)$ is 60 MHz; the length of window $g(L)$ is 120; where as STFT vector is of length $M = 60$ at the output of filter bank. Thus the same DFT resolution is achieved over 60-point DFT in range and 40 point DFT in cross-range. The diagonal elements of $V_r((n-m), \omega_q)$ repeat at 6 DFT bins interval in fast time and 3 DFT bins in slow time. Fig.6 shows the result of coarse resolution IRF processing for a single range-cross-range line of return signal.

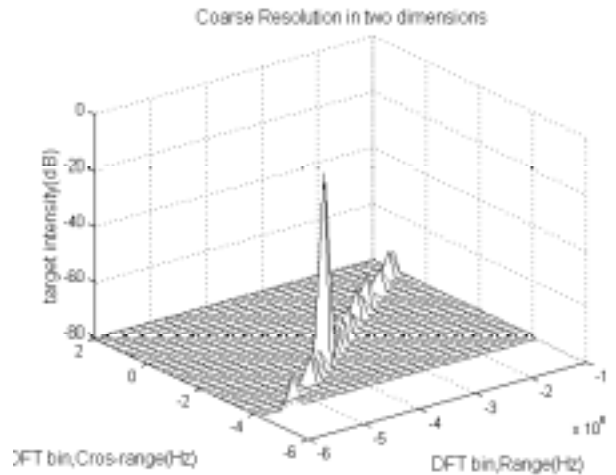


Fig.6. Coarse resolution analysis for three adjacent bins

Three point targets are chosen around phase center in range and cross-range in adjacent bins. It is seen that response for three adjacent targets are merged together due to smaller time duration of subaperture in the coarse resolution case. They are resolved as a single point target response limited by the resolution of coarse DFT bin. The same three targets are resolved separately for fine resolution in Fig.7 representing the fully focused case. This is the case when resolution bandwidth of coarse DFT bin is sampled finely at the rate of fully focused bandwidth.

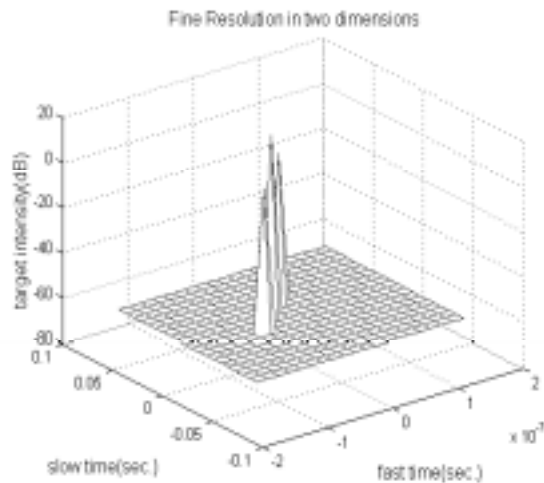


Fig.7. Fine resolution analysis for three adjacent Targets

Multilook processing is the non-coherent (squared magnitude) average of coarse resolution analysis.

IV. Conclusion

Polyphase filterbank interpretation of step transform in SAR image formation is presented here. This model of image formation is suitable for real-time image formation for airborne sensors offering two levels of resolution. The simplifications assumed from real life scenario can be modified at appropriate stages of the model without altering the basic approach of image formation as shown in [1],[10].

Acknowledgement: The author is thankful to Dr. A. Kar and Dr.J. Roy of Jadavpur University, Kolkata for their help in shaping the idea of the paper. The kind permission of Director, DEAL, to submit the paper is acknowledged.

References

- [1] C. Cafforio, C. Prati and F. Rocca, "SYNTHETIC APERTURE RADAR FOCUSING WITH POLYPHASE FILTERS" *Signal Processing*, vol.18, 1989, pp.397-411
- [2] V.C. Chen and S. Qian, "Joint Time -Frequency Transform for Radar Range- Doppler Imaging," *IEEE Trans. AES*, vol.34, No.2, 1998, pp.486-499
- [3] J.C. Curlander and R.N. McDonough, *Synthetic Aperture Radar, Systems and Signal Processing*, chapter10: John Wiley & Sons, Inc., 1991
- [4] N.J. Fliege, *Multirate Digital Signal Processing*, John Wiley & Sons Ltd., 1994
- [5] R. Lanari, S. Hensley and P.A. Rosen, "Chirp z-transform based SPECAN approach for phase - preserving ScansAR image generation," *IEE Proc.- Radar, Sonar Navig.*, vol.145, No.5, 1998, pp.254-261
- [6] A. Moreira, "Real- Time Synthetic Aperture Radar (SAR) Processing with a New Subaperture Approach," *IEEE Trans. Geosci. and Remote Sensing*, vol.30, No.4, 1992, pp.714-722
- [7] A. Moriera, T. Misra and S. Chowdhury, "Modelling and Performance Evaluation Of A New Subaperture Approach For Real-time SAR Processing," *IEE Proc., Radar'92*, pp.399-402
- [8] D.C. Munson and R.C. Visentin, "A Signal Processing View of Strip-Mapping Synthetic Aperture Radar," *IEEE Trans. ASSP*, vol.37, No.12, 1989, pp.2131-2147
- [9] R.P. Perry, R.C. Dipietro, B.L. Johnson, A. Kozma and J.J. Vaccaro, "Planar Subarray Processing for SAR Imaging," *Proc. IEEE Radar Conf.*, 1995, pp. 473-478
- [10] M. Sack, M.R. Ito and I.G. Cumming, "Application of efficient linear FM matched filtering algorithms to synthetic aperture radar processing," *IEE Proc.*, Pt.F, vol.32, 1985, pp.45-57
- [11] X. Sun, T. S. Yeo, C. Zhang Y. Liu and P. S. Kooi, "Time-Varying Step- Transform Algorithm for High Squint SAR Imaging," *IEEE Trans. Geosci. and Remote Sensing*, vol.37, No.6, Nov.1999, pp.2668-2677
- [12] B. Walker, G. Sander, M. Thompson, R. Fellerhoff, D. Dubbert, A High -Resolution, Four-Band SAR Testbed with Real-Time Image Formation, <http://www.sandia.gov/radar/>
- [13] A. Vidal-Pantaleoni and M. Ferrando, "A New Spectral Analysis Algorithm for SAR Data Processing of ScanSAR Data and Medium resolution Data without Interpolation," *Proc. IGARSS*, vol. I, 1998, pp.639-641